JOURNAL OF MATERIALS SCIENCE LETTERS 19 (2000) 201–203

A differential scanning calorimetry study of aluminum alloy 6111 with different pre-aging treatments

W. F. MIAO, D. E. LAUGHLIN
Department of Materials Science and Engineering, Carnegie Mellon University, Pittsburgh, PA 15213, USA

Age-hardenable Al-Mg-Si(-Cu) alloys have attracted increasing attention in recent years [1–3], partly due to the demand for lighter vehicles as part of the overall goal to improve fuel efficiencies and reduce vehicle emissions. The strengthening of Al-Mg-Si(-Cu) alloys in automotive applications is usually realized through precipitation hardening occurring during the automotive paint bake cycle with an average temperature of 175°C and typical duration of about 20 min. Unfortunately, the paint bake cycle always leaves the alloys in an underaged condition. In addition, for most Al-Mg-Si(-Cu) alloys, the hardening response during artificial aging is adversely affected by natural aging, i.e. the practically unavoidable delay between solution treatment and artificial aging [4–6]. Previous studies [2, 5] have shown that a suitable pre-aging procedure, i.e. aging at an intermediate temperature immediately after solution treatment, is effective in reducing the detrimental effects of natural aging on the artificial aging response during the paint bake cycle. However, due to the difficulties related to the observation of ultrafine clusters or zones formed during pre-aging treatments by the use of electron microscopy techniques, the understanding of the underlying mechanisms is far from complete. In this study, differential scanning calorimetry has been used in conjunction with hardness measurements and transmission electron microscopy to investigate the effects of different pre-aging treatments on the precipitation behavior in an aluminum alloy 6111.

The composition of the alloy used in this study was Al-0.54Mg-0.55Si-0.69Cu-0.29Fe-0.1Mn (in wt%). The alloy was solution treated for 20 min at 560°C and quenched in cold water. After quenching, samples were subjected to two different thermal treatments. In the first treatment, samples were kept at room temperature for 30 days. In the second treatment, a pre-aging at 75°C for 8 h, followed by 30 days of room temperature storage was imposed. Differential scanning calorimetry (DSC) analysis of the samples was performed in a Perkin-Elmer DSC-7. During the DSC measurements, the samples were protected with flowing argon. A high purity Al sample of the similar mass to that of the specimen was used as reference. Rockwell 15T hardness measurements were carried out in a Wilson hardness tester. Transmission electron microscopy (TEM) was carried out in a Philips TM420 microscope operating at 120 kV. TEM specimens were prepared by jet-polishing in 30 vol% HNO_3–70 vol% CH_3OH solution at −20 to −30°C.

Fig. 1 shows the DSC curve, taken at a heating rate of 20°C min^{-1}, of an as-quenched sample and the corresponding hardness curve. The hardness data were obtained from samples heated to the corresponding temperatures on the DSC curve at a heating rate of 20°C min^{-1} and kept there for 1 min before quenching to room temperature. Based on the previous DSC investigations of Al-Mg-Si(-Cu) alloys [2, 3, 7], the peaks on the DSC curve of the as-quenched sample can be correlated to the precipitation process as follows: the exothermic peaks centered at around 100°C and 250°C are caused by GP zone or cluster formation and β'' precipitation, respectively. The exothermic peak at around 300°C should correspond to β' and/or Q′ precipitation [3, 8]. It is seen that the hardness increased with increasing temperature until a maximum was reached at around 250°C. This indicated that although the formation of GP zones certainly hardened the alloy, the β'' precipitates are more effective in strengthening the alloy. In addition, the fact that no hardness reduction was observed between GP zone formation and β'' precipitation suggests that no GP zone dissolution occurred. The precipitation of β' and/or Q′ is mainly responsible for the decrease in hardness at higher temperatures.

Fig. 2 displays the DSC curve taken at a heating rate of 20°C min^{-1} and the corresponding hardness curve of a sample naturally aged for 30 days. Unlike the DSC curve of the as-quenched sample, the DSC curve of the naturally aged sample did not show any exothermic behavior at around 100°C. Instead, a very broad endothermic bump appeared between 140°C and 230°C. The

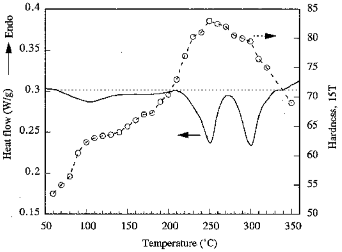

Figure 1 DSC trace (scan rate 20°C min^{-1}) and the corresponding hardness plot for as-quenched aluminum alloy 6111.

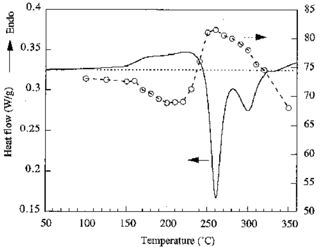

Figure 2 DSC curve (scan rate 20°C min^{-1}) and the corresponding hardness plot for a sample naturally aged for 30 days.

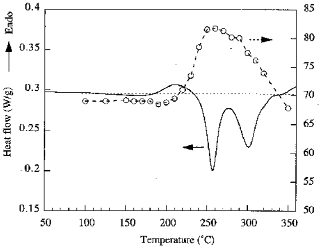

Figure 3 DSC trace (scan rate 20°C min^{-1}) and the corresponding hardness curve for a sample pre-aged at 75°C for 8 h followed by 30 days of natural aging.

disappearance of the exothermic peak around 100°C indicates that GP zones already existed in the naturally aged sample. The broad endothermic bump is accompanied by a harness reduction, indicating that at least some of the GP zones in the naturally aged sample dissolved during the heating. The broadness of the bump suggests that different kinds of zones/clusters existed in the naturally aged sample, or that the sizes of the zones/clusters in the naturally aged samples are far from being uniform. With the precipitation of β'', the hardness began to increase. Again, the precipitation of β' and/or Q$'$ caused a reduction in hardness.

Fig. 3 presents the DSC trace (scan rate 20°C min^{-1}) and the corresponding hardness curve of a sample pre-aged at 75°C for 8 h followed by 30 days natural aging. The disappearance of the GP zone formation peak and the presence of β'' precipitation peak indicates that GP zones not β'' existed in the pre-aged sample. On the DSC curve, no endothermic peaks were observed below 180°C either, suggesting that the zones or clusters formed during pre-aging and subsequent natural aging are more stable than those in the naturally aged sample. This is in accordance with the hardness data where essentially no hardness drop was observed for the pre-aged sample until 180°C. However, an endothermic bump did exist on the DSC curve between 180°C and

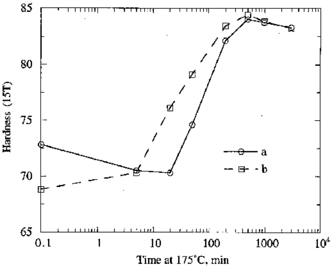

Figure 4 Variation of hardness with artificial aging time at 175°C for samples (a) naturally aged for 30 days, (b) pre-aged at 75°C for 8 h followed by 30 days of natural aging.

230°C. This relatively small bump was accompanied by a slight hardness decrease, indicating a dissolution of some of the pre-existing zones. However, compared with those of the naturally aged sample (Fig. 2), both the heat absorbed during the dissolution and the degree of hardness reduction were much smaller.

Fig. 4 shows the artificial aging response at 175°C for the sample pre-aged at 75°C for 8 h followed by 30 days of natural aging. Also shown in Fig. 4 is the artificial aging response for the samples naturally aged for 30 days only. For the naturally aged sample, there was a hardness decrease in the initial artificial aging stage. This is thought to be caused by the dissolution of the pre-existing zones, as was evident from the endothermic bump on the corresponding DSC curve (see Fig. 2). On the other hand, the sample pre-aged at 75°C for 8 h followed by 30 days of natural aging did not show any hardness reduction in the same initial artificial aging period. Although the peak hardnesses were more or less the same, the artificial aging kinetics was significantly enhanced by the pre-aging treatment at 75°C. For the condition currently of most interest to the automotive applications (20 min at 175°C), the hardness of the pre-aged sample was considerably higher than that of the naturally aged counterpart (~76 vs. ~70).

Fig. 5 shows the bright field TEM micrographs and the corresponding $[001]_{Al}$ selected area electron diffraction patterns of samples artificially aged at 175°C for 20 min after different pre-aging treatments. For the naturally aged sample, artificial aging at 175°C for 20 min did not produce any distinguishable features of precipitates in either the bright field image or the diffraction pattern. On the other hand, for the sample pre-aged at 75°C for 8 h, after being artificially aged at 175°C for 20 min, the micrograph reveals the presence of dot-like precipitates. The streaks along $[010]_{Al}$ and $[001]_{Al}$ directions on the diffraction pattern indicate that the precipitates are needle-like β'' along $\langle 001\rangle_{Al}$ directions. The dot-like precipitates are needles viewed end-on. However, largely due to very small strain contrast since these precipitates are fully coherent with the matrix along their long axis [9], needles along $[100]_{Al}$ and $[010]_{Al}$ directions are not clearly visible.

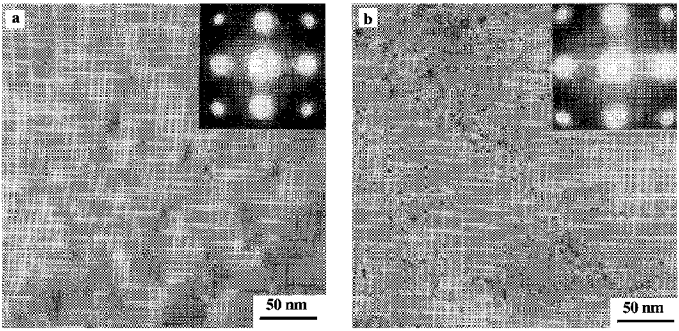

Figure 5 Bright field TEM micrographs and the corresponding $[001]_{Al}$ selected area diffraction patterns of samples artificially aged at 175°C for 20 min after (a) being naturally aged for 30 days, (b) pre-aged at 75°C for 8 h followed by 30 days of natural aging.

TEM investigations of the sample naturally aged for 30 days and the sample pre-aged at 75°C for 8 h followed by 30 days of natural aging failed to find evidence of any precipitation. Nevertheless, based on DSC results and previous studies [3, 10], ultrafine GP zones or clusters should exist in both samples. However, the DSC and hardness measurements suggest that the GP zones or clusters in the sample naturally aged for 30 days only are less stable than those in the sample pre-aged at 75°C for 8 h followed by 30 days of natural aging. Therefore, the sizes of a significant part of the GP zones in the naturally aged sample must be subcritical and would dissolve in the early stage of subsequent artificial aging at 175°C. On the other hand, most of the GP zones in the pre-aged sample should be stable enough to act as nuclei for β'' precipitation during subsequent artificial aging.

In conclusion, pre-aging treatments impose a significant effect on the precipitation hardening behavior of aluminum alloy 6111. In particular, the results of this study show that the GP zones formed during natural aging and pre-aging at 75°C for 8 h differ in size and/or structure. During subsequent artificial aging, a reversion process exists for the GP zones or clusters in the naturally aged sample. On the other hand, the GP zones or clusters formed during pre-aging are more stable and can act as nuclei for the precipitation of the main strengthening phase, β'', and hence enhance the artificial aging response.

Acknowledgments
The authors are grateful to Dr. David J. Lloyd at Alcan International Limited for helpful discussions and Mr. E. Chang for technical assistance. WFM was partially supported by a grant from the Ford Motor Company. DEL acknowledges a grant from NEDO.

References
1. A. K. GUPTA, P. H. MAROIS and D. J. LLOYD, *Mater. Sci. Forum* **217–222** (1996) 801.
2. J. D. BRYANT, in "Automotive alloys", edited by S. K. Das and G. J. Kipouros (The Minerals, Metals & Materials Society, 1997) p. 19.
3. G. A. EDWARDS, K. STILLER, G. L. DUNLOP and M. J. COUPER, *Acta Mater.* **46** (1998) 3893.
4. D. W. PASHLEY, J. W. RHODES and A. SENDOREK, *J. Inst. Met.* **94** (1966) 41.
5. L. ZHEN and S. B. KANG, *Scri. Mater.* **36** (1997) 1089.
6. D. E. LAUGHLIN, W. F. MIAO, L. M. KARABIN and D. J. CHAKRABARTI, in "Automotive alloys II", edited by S. K. Das (The Minerals, Metals & Materials Society, 1998) p. 63.
7. I. DUTTA and S. M. ALLEN, *J. Mater. Sci. Lett.* **10** (1991) 323.
8. W. F. MIAO and D. E. LAUGHLIN, research in progress.
9. G. THOMAS, *J. Inst. Metals* **90** (1961–62) 57.
10. K. MATSUDA, T. YOSHIDA, H. GAMADA, K. FUJII, Y. UETANI, T. SATO, A. KAMIO and S. IKENO, *J. Japan Inst. Metals* **62** (1998) 133.

Received 2 March
and accepted 10 August 1999